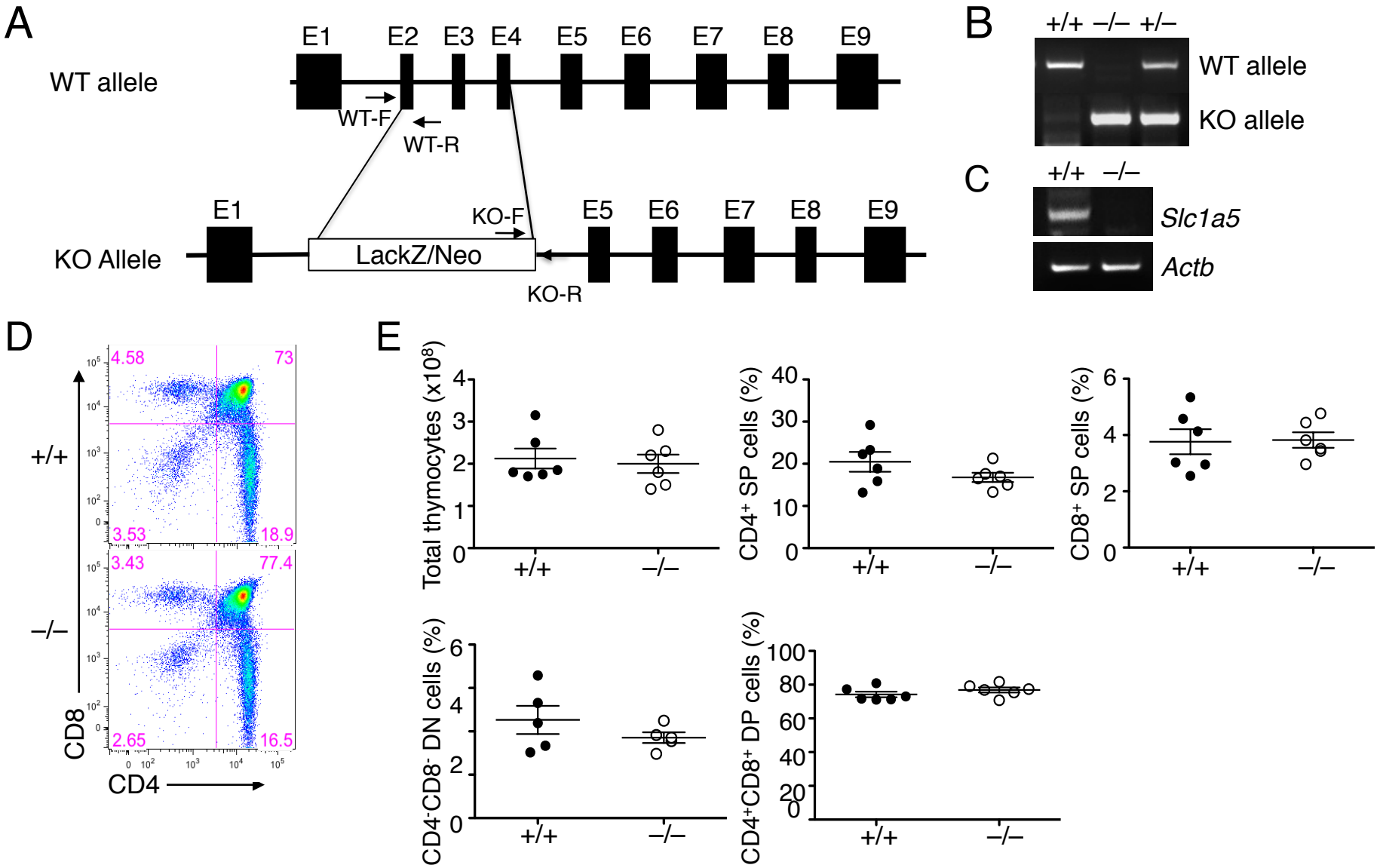

Figure S1. Slc1a5 gene targeting. Related to Figure 1.

(A) *Slc1a5* gene locus and targeting strategy. Exons 2-4 were replaced with a lacZ-neomycin cassette. Forward (F) and reverse (R) genotyping PCR primers for amplifying wild-type (WT) allele (WT-F and WT-R) and knockout (KO) allele (KO-F and KO-R) are indicated.

(B) Genotyping PCR to detect WT (+/+), Slc1a5 heterozygous (+/–) and homozygous (–/–) knockout mice.

(C) RT-PCR to amplify ASCT2 mRNA encoded by exons 8 and 9. *Actb* (β-actin) was used as a loading control.

(D) Flow cytometry analysis of thymocyte sub-populations of young adult (6-7 wk old) Slc1a5$^{+/+}$ and Slc1a5$^{-/-}$ mice. Numbers indicate the percentage of CD4$^+$ (lower right) and CD8$^+$ (upper left) single-positive (SP), CD4$^+$CD8$^+$ double-positive (DP, upper right), and CD4$^-$CD8$^-$ double-negative (DN, lower left) thymocytes.

(E) Total thymocyte number and frequency of the indicated thymocyte sub-populations in *Slc1a5*$^{+/+}$ and *Slc1a5*$^{-/-}$ mice (6-7 wk old). Data are representative of three independent experiments with at least five mice per group.

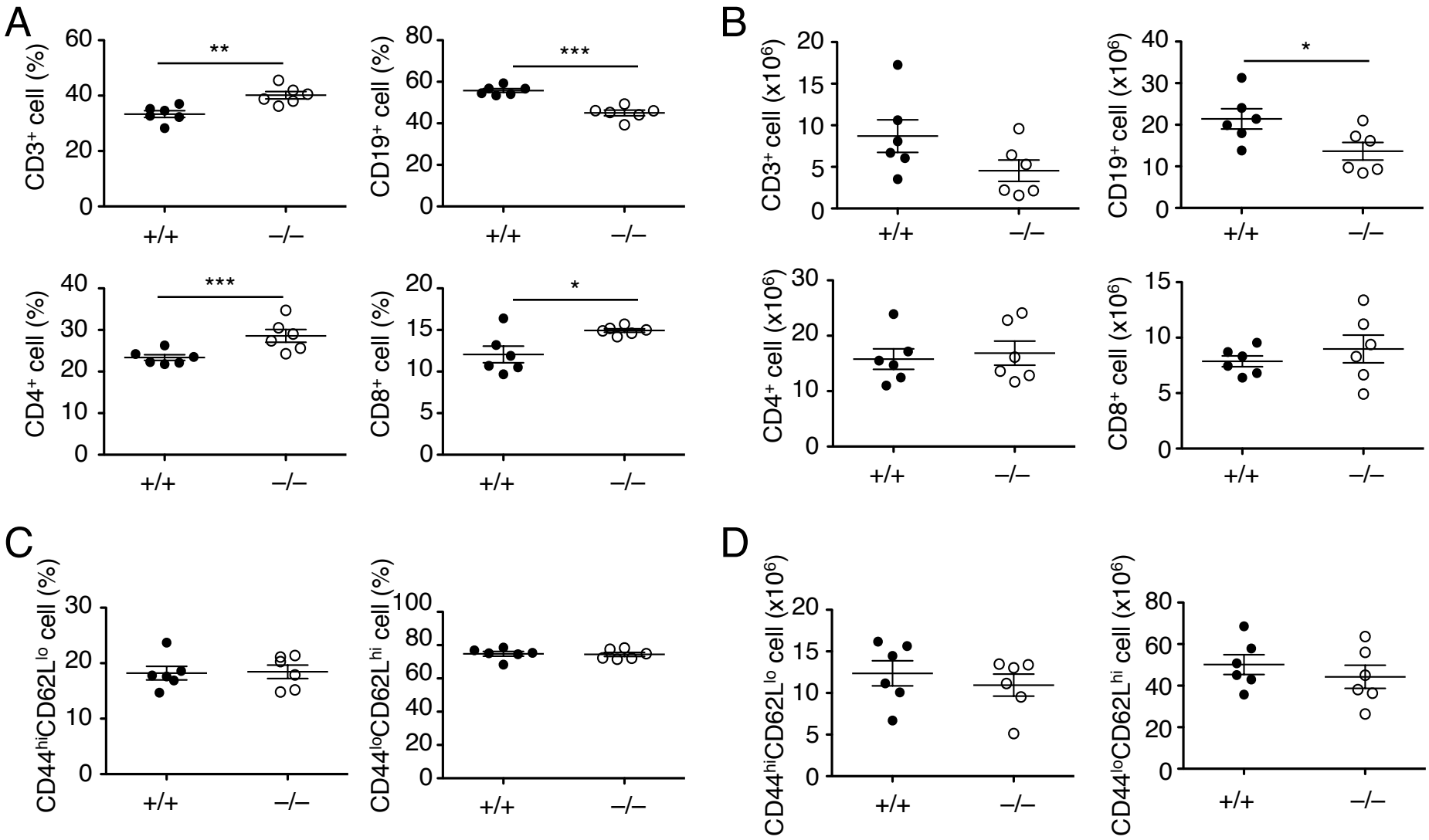

Figure S2. Peripheral lymphocyte profile. Related to Figure 1.

(A and B) Flow cytometry analysis of the frequency (A) and absolute number (B) of total ($CD3^+$), $CD4^+$, and $CD8^+$ T cells and $CD19^+$ B cells in the spleen of young adult (6-7 wk old) *Slc1a5*$^{+/+}$ and *Slc1a5*$^{-/-}$ mice.

(C and D) Flow cytometry analysis of the frequency (C) and absolute number (D) of $CD44^{hi}CD62L^{lo}$ cell in the spleen of young adult (6-7 wk old) of *Slc1a5*$^{+/+}$ and *Slc1a5*$^{-/-}$ mice. Data are representative of three independent experiments with five or more mice per group. **P* < 0.05, ***P* < 0.01, ****P*<0.001.

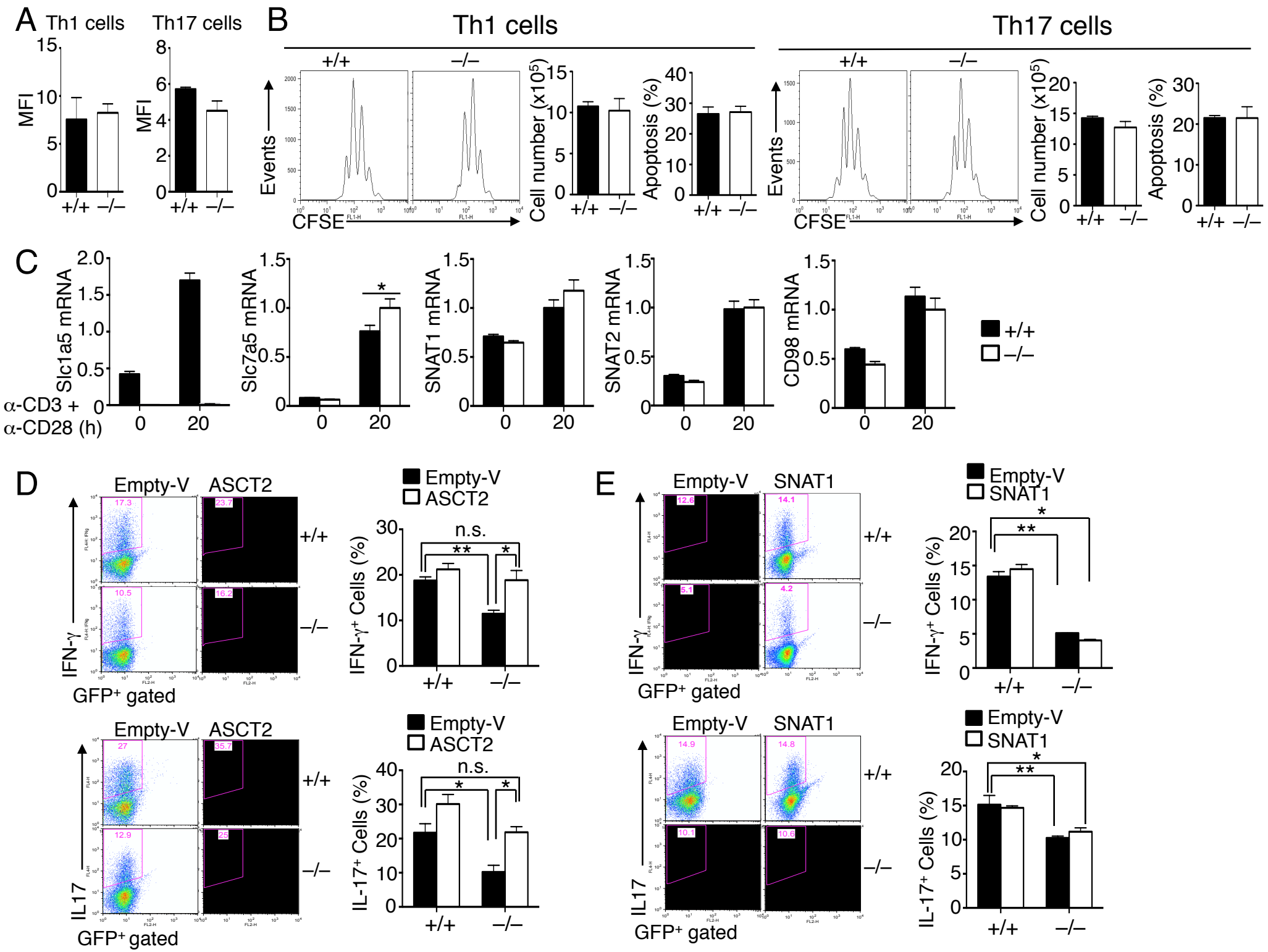
A
Th1 cells
Th17 cells
MFI
+/+
–/–
B
Th1 cells
Th17 cells
Events
CFSE
Cell number (x10^5)
Apoptosis (%)
C
Slc1a5 mRNA
Slc7a5 mRNA
SNAT1 mRNA
SNAT2 mRNA
CD98 mRNA
α-CD3 + α-CD28 (h)
D
Empty-V
ASCT2
IFN-γ
GFP+ gated
IFN-γ+ Cells (%)
IL17
IL-17+ Cells (%)
n.s.
E
SNAT1

Figure S3. ASCT2 is required for T-cell differentiation but not proliferation or survival. Related to Figure 2.

(A) Flow cytometry analysis of median florescence intensity (MFI) of IFN-γ and IL-17 on gated *Slc1a5*$^{+/+}$ and *Slc1a5*$^{-/-}$ Th1 and Th17 cells generated in vitro from *Slc1a5*$^{+/+}$ or *Slc1a5*$^{-/-}$ naïve CD4^{+} T cells (for 4 days).

(B) Naïve CD4^{+} T cells were labeled with CFSE and stimulated under Th1 and Th17 skewing conditions. On day 4, the cells were subjected to proliferation assays based on CFSE dilution and absolute cell number counting, and apoptosis assays based on propidium iodide (PI) and AnexinV staining. Data are representative of three independent experiments with three or more mice per group (mean ± s.d.).

(C) QPCR analysis of relative mRNA levels for the indicated in *Slc1a5*$^{+/+}$ or *Slc1a5*$^{-/-}$ naïve CD4^{+} T cells, stimulated for 20 h with plate-bound anti-CD3 and anti-CD28.

(D and E) Naive CD4^{+} T cells of *Slc1a5*$^{+/+}$ and *Slc1a5*$^{-/-}$ were stimulated with anti-CD3 and anti-CD28 and then infected with GFP-expressing retroviral vectors that either lack a cDNA insert (Empty-V) or encoding ASCT2 or SNAT1. The infected cells were cultured under Th1 and Th17 skewing conditions for 4 days and subjected to flow cytometry analysis to detect the intracellular level of IL-17 and IFN-γ (gated on GFP^{+} cells). Data are representative of three independent experiments with three or more mice per group (mean ± s.d.). **P* < 0.05, ***P* < 0.01.

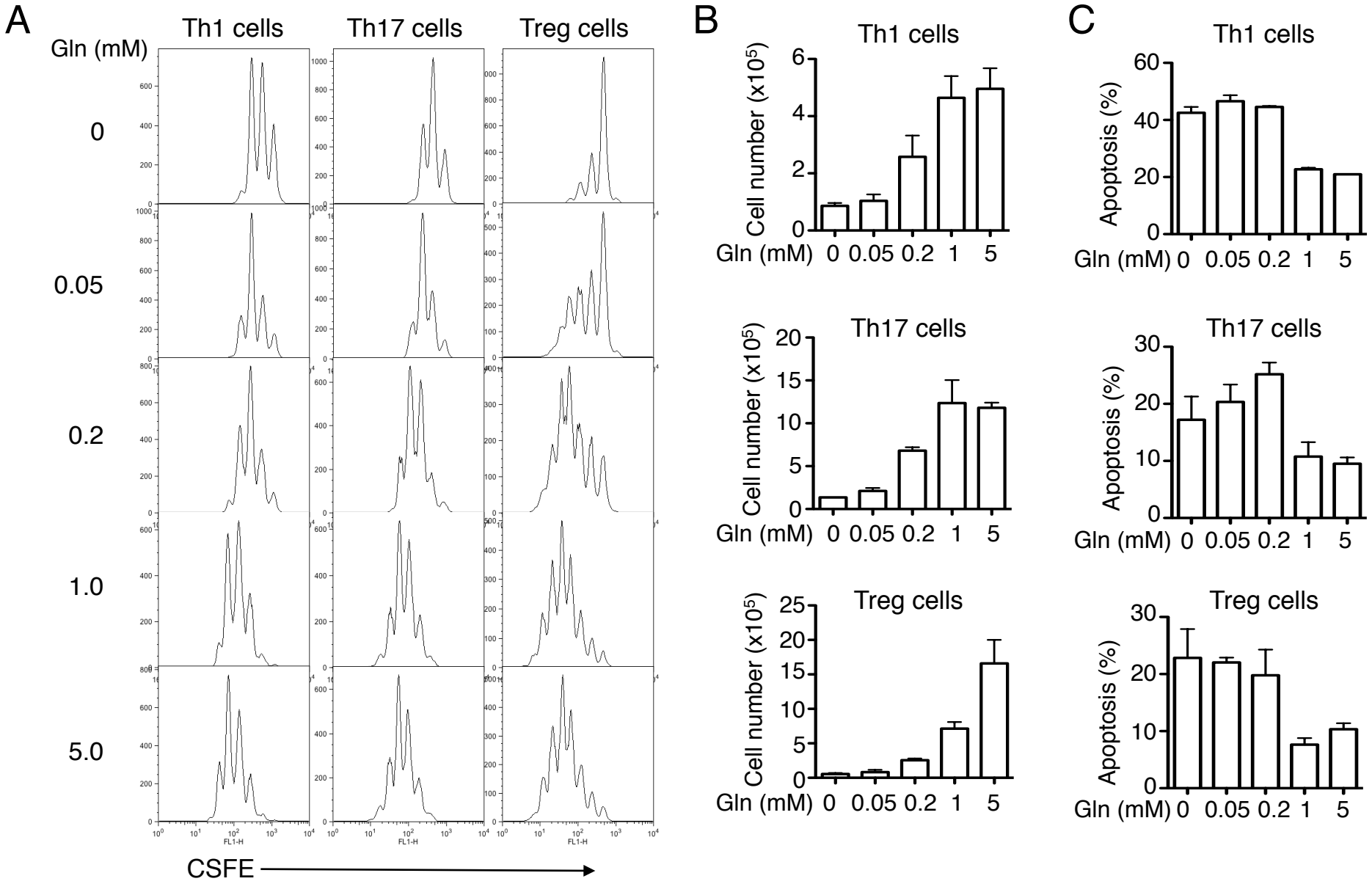

Figure S4. Glutamine is required for CD4$^+$ T cell proliferation. Related to Figure 5.

Naïve CD4$^+$ T cells were labeled with CFSE and stimulated under Th1 and Th17 skewing conditions in glutamine-free medium supplemented with the indicated amount of L-glutamine. On day 4, the cells were analyzed for proliferation based on CFSE dilution (A), absolute cell number counting (B), and apoptosis assay based on staining with PI and AnexinV (C). Data are representative of three independent experiments with three or more mice per group (mean ± s.d.).

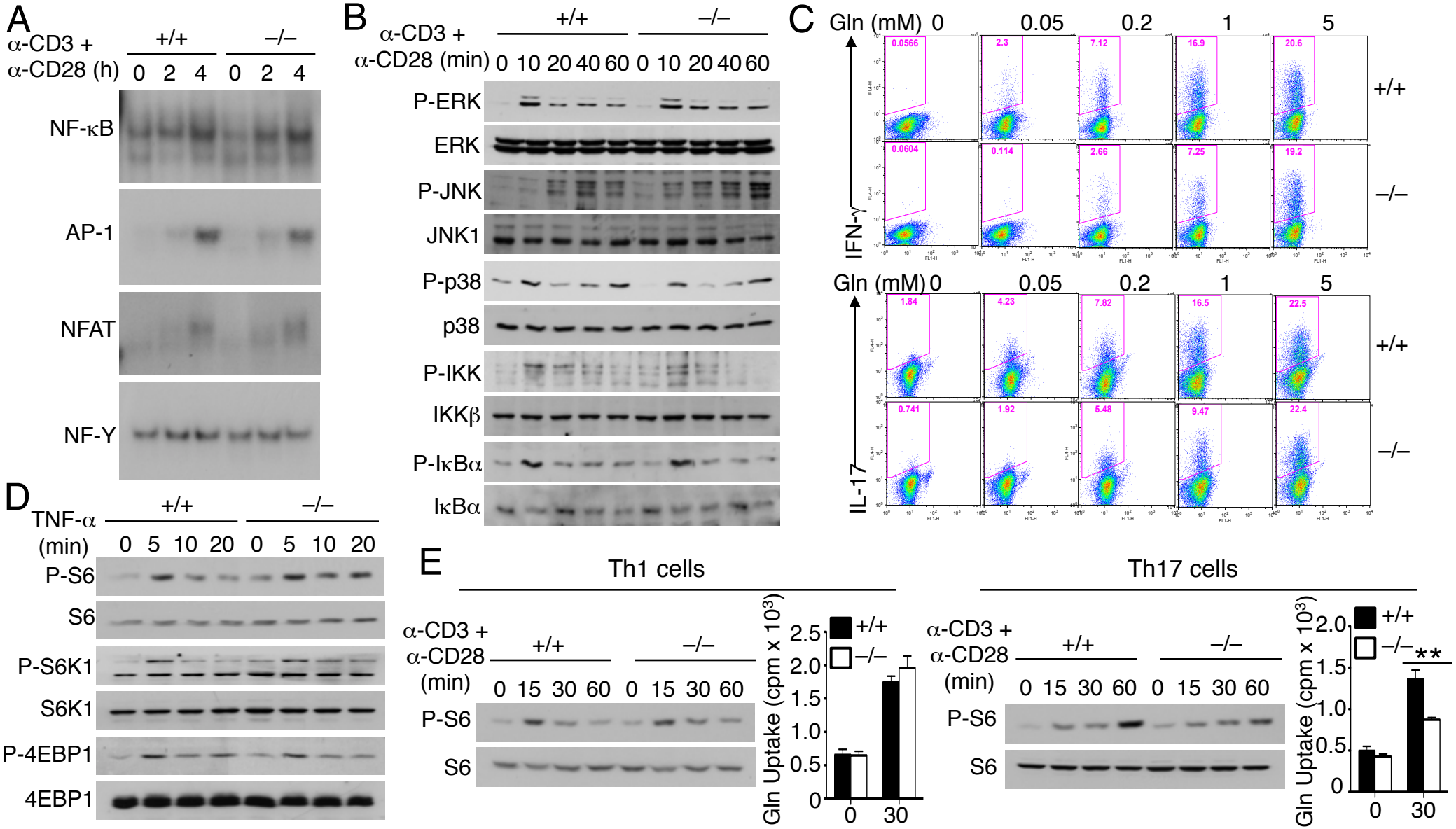

Figure S5. ASCT2 specifically regulates TCR and CD28-stimulated activation of mTORC1 but not other signaling molecules. Related to Figure 6.

(A) EMSA of the inducible transcription factors and the control NF-Y in nuclear extracts of *Slc1a5*$^{+/+}$ or *Slc1a5*$^{-/-}$ naïve CD4^{+} T cells, stimulated with plate-bound anti-CD3 and anti-CD28 for the indicated time periods.

(B) IB analyses of the indicated phosphorylated (P-) and total proteins in whole-cell lysates of *Slc1a5*$^{+/+}$ or *Slc1a5*$^{-/-}$ naïve CD4^{+} T cells, stimulated with anti-CD3 and anti-CD28 using the crosslinking method.

(C) Flow cytometry analysis of Th1 and Th17 cells generated thorough in vitro differentiation of *Slc1a5*$^{+/+}$ or *Slc1a5*$^{-/-}$ naïve CD4^{+} T cells (for 4 days) under the polarizing conditions in glutamine-free medium supplemented with the indicated amount of L-glutamine.

(D) IB analyses of the indicated phosphorylated (P-) and total proteins in whole-cell lysates of *Slc1a5*$^{+/+}$ or *Slc1a5*$^{-/-}$ naïve CD4^{+} T cells, stimulated with TNF-α.

(E) IB analyses of phosphorylated (P-) and total S6 (left) and glutamine uptake analysis (right) of in vitro differentiated *Slc1a5*$^{+/+}$ or *Slc1a5*$^{-/-}$ Th1 and Th17 cells, stimulated with anti-CD3 and anti-CD28 using the crosslinking method. Data are representative of three independent experiments with at least three mice per group. $^{**}P < 0.01$.

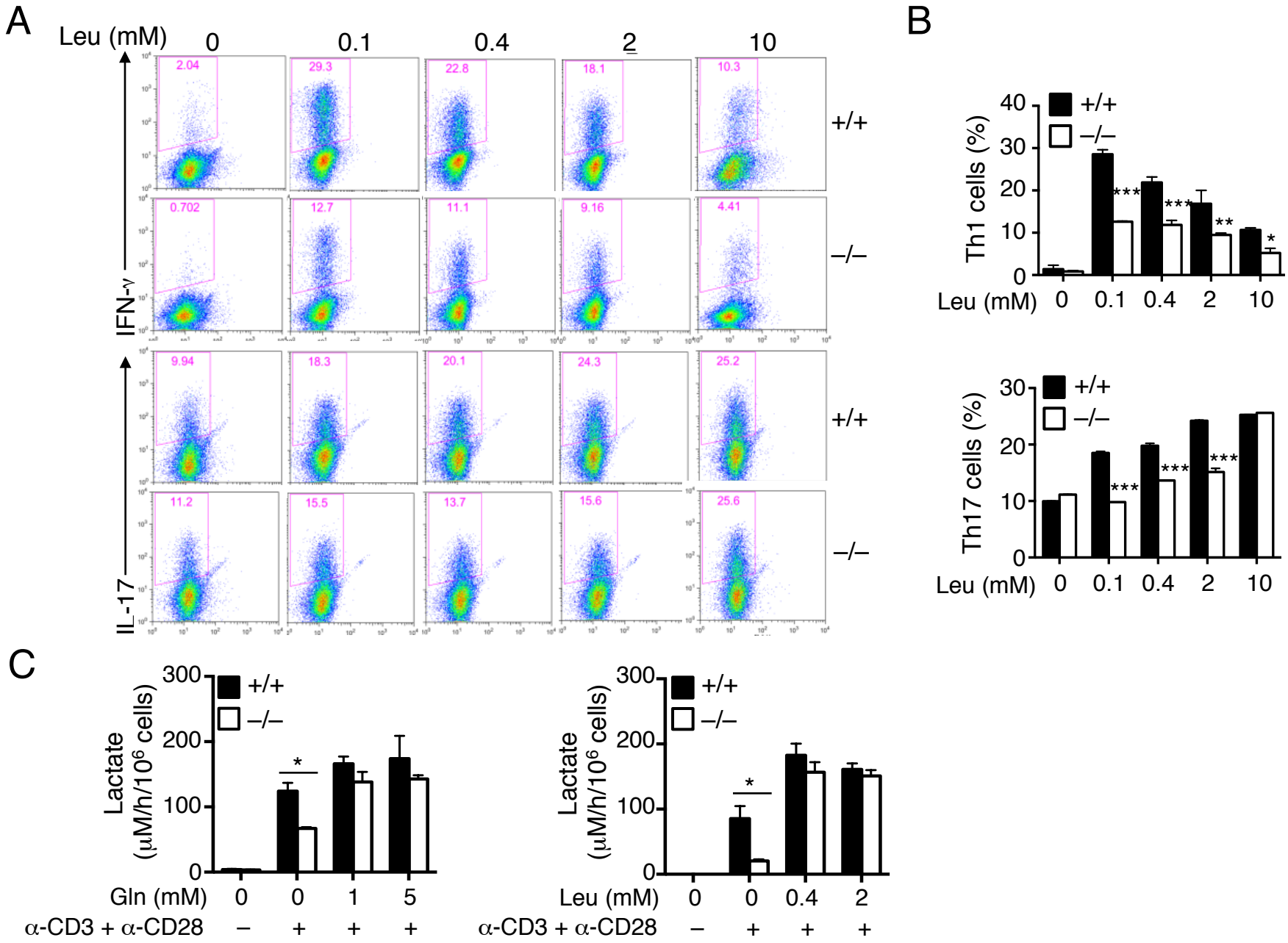

Figure S6. Effect of excessive leucine on T-cell differentiation and glycolysis. Related to Figure 6.

(A and B) Flow cytometry analysis of Th1 and Th17 cells generated thorough in vitro differentiation of *Slc1a5*$^{+/+}$ or *Slc1a5*$^{-/-}$ naïve CD4^{+} T cells (for 4 days) under the polarizing conditions in leucine-free medium supplemented with the indicated amount of L-leucine. Data are presented as a representative FACS plot (A) or mean ± s.d. (B) of three independent experiments with least four mice per group.

(C) *Slc1a5*$^{+/+}$ or *Slc1a5*$^{-/-}$ naïve CD4^{+} T cells were either not treated (–) or stimulated (+) with plate-bound anti-CD3 plus anti-CD28 for 20 h in a 96-well plate in the presence of the indicated concentrations of glutamine (Gln) or leucine (Leu). Lactate concentration in the culture medium was measured and calculated as described in the Extended Experimental Procedures. **P* < 0.05, ***P* < 0.01, ****P*<0.001.

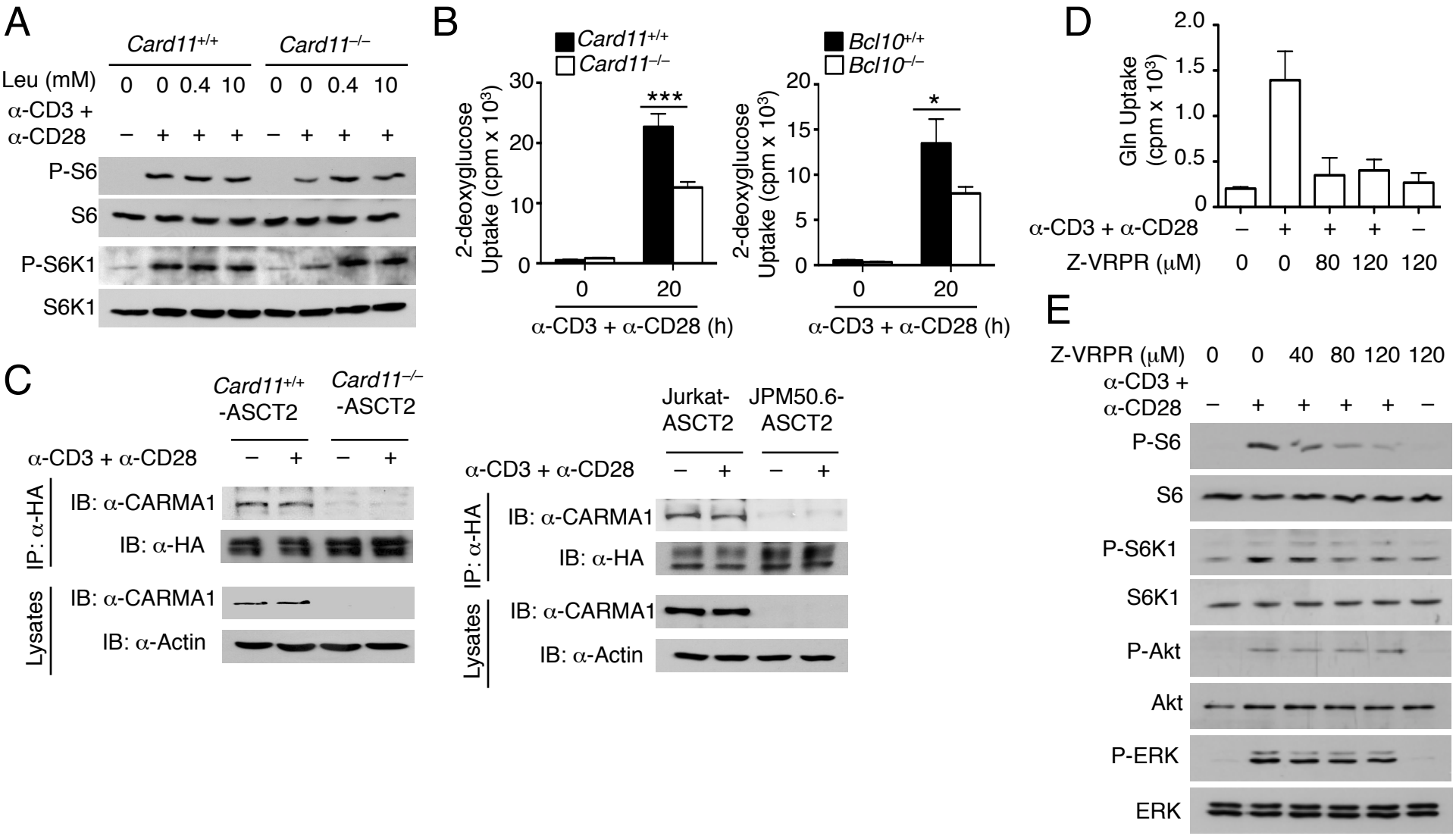

Figure S7. Role of CBM complex in the regulation of glutamine and glucose uptake and mTORC1 signaling. Related to Figure 7.

(A) IB analyses of the indicated phosphorylated (P-) and total proteins in whole-cell lysates of *Slc1a5*$^{+/+}$ or *Slc1a5*$^{-/-}$ naïve CD4$^+$ T cells, stimulated with anti-CD3 and anti-CD28 using the crosslinking method in leucine-free medium supplemented with the indicated amount of L-leucine.

(B) 2-deoxyglucose uptake analysis of naïve CD4$^+$ T cells from the indicated mice, stimulated for 20 h with plate-bound anti-CD3 and anti-CD28 in glucose-free medium.

(C) Primary *Card11*$^{+/+}$ and *Card11*$^{-/-}$ T cells or Jurkat and JPM50.6 cells were transduced with the HA-ASCT2 retroviral vector. The cells were either not treated (–) or stimulated (+) with anti-CD3 and anti-CD28 using the crosslinking method for 30 min. ASCT2 was isolated by IP using anti-HA, and its associated CARMA1 was detected by IB (upper). The expression of ASCT2 and CARMA1 was monitored by direct IB (lower).

(D and E) Glutamine uptake (D) and IB (E) analysis of WT naïve CD4$^+$ T cells, stimulated as described in A in the presence of the indicated concentrations of a MALT1 inhibitor, Z-VRPR.

Data are representative of three independent experiments with three or more mice per group (mean ± s.d. in B and D). *$P < 0.05$, **$P < 0.01$.

Genotyping PCR primers

Allele	Forward primer	Reverse primer
WT allele	CATTGCCACTCTCCAGGAAG	GCCGTTCATGCCAGTTTCACTTATTGAG
KO allele	GGTGTGGCGGACCGCTATCAGGAC	GAAGACTCAAACAACAGAGGG

RT-PCR primer

Gene	Forward primer	Reverse primer
ASCT2	GAAGACTCAAACAACAGAGGG	TCCTCTGTGGCGAGGGGCAG
Actb	CGTGAAAAGATGACCCAGATCA	CACAGCCTGGATGGCTACGT

QPCR primer

Gene	Forward primer	Reverse primer
ASCT2	TGCTTTCGGGACCTCTTCTA	TGATGTGTTTGGCCACACCA
Slc7a5	CTGGATCGAGCTGCTCATC	GTTCACAGCTGTGAGGAGC
CD98	CAAAGTGCCAAGAAAAAGAGC	CTGAGCAGGGAGGAACCAC
SNAT1	TTACCAACCATCGCCTTC	ATGAGAATGTCGCCTGTG
SNAT2	GGTATCTGAACGGTGACTATCTG	TCTGCGGTGCTATTGAATGC
IFNg	CAGCAACAGCAAGGCGAAA	CTGGACCTGTGGGTTGTTGAC
IL-4	CGCCATGCACGGAGATG	CGAGCTCACTCTCTGTGGTGTT
IL-17A	CTCAGACTACCTCAACCGTTC	TGAGCTTCCCAGATCACAGAG
Actb	CGTGAAAAGATGACCCAGATCA	CACAGCCTGGATGGCTACGT

Table S1. Oligonucleotide primers used for genotyping of *ASCT2*-KO mice, *ASCT2* RT-PCR and QPCR assays. Related to Experimental Procedures.

EXTENDED EXPERIMENTAL PROCEDURES

Cell lines

Human embryonic kidney cell line 293T was cultured in DMEM media containing 5% FBS and transfected in 6-well plates using the calcium phosphate method. The CARMA1-deficient Jurkat T cell line, JPM50.6, and the parental Jurkat cell line were described previously (Wang et al., 2002).

Plasmids, antibodies and reagents

The retroviral vector pCLXSN(GFP) has been described previously (Reiley et al., 2005), and the pMIGR1-IRES-GFP vector was provided by Dr. Yongwon Choi (King et al., 2006). Human ASCT2 and SNAT1 were cloned into the pCLXSN(GFP) and pMIGR1-IRES-GFP, respectively. Expression vectors encoding Myc-tagged CARMA1 and BCL-10 (in pRK6 vector) and the pcDNA-FLAG-MALT1 were as described (Che et al., 2004; Wang et al., 2002). Anti-CD3 (145-2C11), anti-CD28 (37.51) and anti-IFN-γ (XMG1.2) were from eBioscience, and anti-IL-4 (11B11) was from National Cancer Institute Preclinical Repository. Antibodies for S6, phospho-S6 (Ser235/Ser236), p70 S6 kinase (called S6K1 in this study), phospho-p70 S6 kinase (Thr389), 4E-BP1, phospho-4E-BP1 (Thr37/46), phospho-Akt (Ser473), phospho-JNK (Thr183/Tyr185), phospho-p38 (Thr180/Tyr182), phospho-IKKα/β (Ser176/180), phospho-IκBα (Ser32), and CARD11 (1D12) were from Cell signaling. Antibodies for Akt (B1), phospho-ERK (E4), ERK (K-23), JNK (C-17), p38 (H147), IKKα/β (H470), Gult1 (A4), c-Myc (9E10) (for detection of tagged proteins), β-Actin (C-2) were from Santa Cruz. Anti-HA (12A5) and HRP-

conjugated anti-HA (3F10) were from Roche Molecular Biochemicals. The anti-c-Myc and HRP-conjugated anti-FLAG antibodies were from Invitrogen and Sigma, respectively. Phorobl 12-myriatate 13-acetate (PMA), ionomycin, perchloric acid, and 1-bromododecane were from Sigma. [^{3}H]thymidine and L-2,3,4- [^{3}H]glutamine, [^{3}H]leucine, [^{3}H]phenylalanine and [^{3}H]2-deoxyglucose were from PerkinElmer. The recombinant mouse cytokines IL-12, IL-6, and TGF-β were from R&D systems.

Flow cytometry and cell sorting

Flow cytometry and cell sorting were done as described (Reiley et al., 2006) with a FACSCalibur (BD Bioscience) and FACSAria (BD bioscience), respectively. Fluorescence-labeled antibodies for CD3 (145-2C11), CD4 (GK1.5), CD8α (53-6.7), CD11b (M1/70), CD19 (eBio1D3), CD25 (PC61.5), CD44 (1M7), CD45RB (C363.16A), and CD98 (RL388) were from eBiosciense, and the anti-CD62L (MEL-14) was from BD Biosciense. Intracellular staining using anti-Foxp3 (FJK-16S) was done according to the manufacturer's instructions (eBioscience). For intracellular cytokine staining, the cells were stimulated for 4-6 h with PMA (50 ng/ml) and ionomycin (500 ng/ml) in the presence of monensin (1:1000) before being stained with anti-IL-17 (eBio17B7) and anti-IFN-γ (XMG1.2) according to the manufacturer's instructions (BD Biosciences). Flow cytometry data were analyzed with FlowJo software (Treestar).

***In vitro* T-cell activation**

Purified naïve CD4$^+$ T cells were stimulated with either plate-bound anti-CD3 (5 μg/ml) and anti-CD28 (1 μg/ml) or a crosslinking method. For the crosslinking method, which

was used when analyzing the rapid signaling events, naïve $CD4^+$ T cells were incubated at 37ºC for 30 min and then stimulated for the indicated time periods with anti-CD3 (1 μg/ml) and anti-CD28 (2 μg/ml) that had been premixed with 10 μg/ml of a secondary crosslinking antibody: goat anti-hamster immunoglobulin G (H+L) (Southern Biotech).

***In vitro* T-cell differentiation, T-cell proliferation, and apoptosis assays**

Purified naïve $CD4^+$ T cells ($CD4^+CD44^{lo}CD62L^{hi}$) were activated with plate-bound anti-CD3 (5 μg/ml) and anti-CD28 (1 μg/ml) in RPMI medium supplemented with 10% FBS under Th1 (5 μg/ml IFN-γ, 10 ng/ml IL-12, 5 μg/ml anti-IL-4), Th2 (10 ng/ml IL-4, 5 mg/ml anti-IFN-γ), Th17 (20 ng/ml IL-6, 2.5 ng/ml TGF-β, 5 μg/ml anti-IL-4, 5 μg/ml anti-IFN-γ), or Treg (5 μg/ml anti-IL-4, 5 μg/ml anti-IFN-γ and 2.5 ng/ml TGF-β) conditions. In experiments to examine the effect of glutamine or leucine on T-cell differentiation, the naïve $CD4^+$ T cells were activated in a glutamine-free or leucine-free RPMI medium. After 4 days of activation, the differentiated T cells were re-stimulated for 4 h with PMA and ionomycin in the presence of the protein transport inhibitor monensin, followed by intracellular staining of IFN-γ, IL-17, and Foxp3 to quantify the frequency of Th1, Th17, and Treg cells.

For T-cell proliferation assays, the stimulated T cells were pulse-labeled for 6 h with [^{3}H]thymidine, and the proliferation was measured based on thymidine incorporation. In some experiments, cell proliferation was also performed based on the dilution of CFSE (carboxyl fluorescent succinimidyl ester) dilution (Chang et al., 2011). Apoptosis was quantified by flow cytometry based on staining with Propidium Iodide and AnexinV according to the manufacturer's instructions (BD Bioscience).

Enzyme-linked immunosorbent assay (ELISA), glutamine concentration, oxygen consumption analysis and lactate measurement

Purified naïve $CD4^+$ T cells ($CD4^+CD44^{lo}CD62L^{hi}$) were stimulated with plate-bound anti-CD3 and anti-CD28. After the indicated times of stimulation, cell culture supernatants were collected for ELISA assays (eBioscience) to measure the concentration of cytokines. For measurement of intracellular glutamine concentration, the cells were lysed with RIPA buffer (50 mM Tris-HCl, pH 7.4, 150 mM NaCl, 1% (vol/vol) Nonidet P-40, 0.5% (vol/vol) sodium deoxycholate and 1 mM EDTA) and deproteinated with 1/20 volume of 100% trichloroacetic acid (Buschdorf et al., 2006; Kung et al., 2011). Glutamine concentration in the cell lysates was determined using the GLN-1 kit (Sigma).

Oxygen consumption rate was measured using a commercial kit (Cayman Chemical) according to the manufacturer's instructions and a previous report (Hynes et al., 2006). Purified naïve $CD4^+$ T cells ($CD4^+CD44^{lo}CD62L^{hi}$) were stimulated with plate-bound anti-CD3 and anti-CD28 in a 96-well plate at a density of 10^6 cells/well. After 20 h, the cell culture was changed with fresh media containing a fluorescence probe, and the plate was placed in a fluorescence signal plate reader and monitored for 120 min. Instrument setting was 380 nm of excitation filter and 650 nm of emission filter with a delay time of 30 μs and a gate time of 100 μs.

Lactate production was measured using a commercial kit (Abcam) according to manufacturer's instructions and previous report (Finlay et al., 2012). Purified naïve $CD4^+$ T cells ($CD4^+CD44^{lo}CD62L^{hi}$) were cultured in medium containing 10% dialyzed FBS and stimulated with plate-bound anti-CD3 and anti-CD28 in a 96-well plate at a density

of 10^6 cells/well. After 20 h, supernatants were collected and concentration of lactate was calculated by standard curve and presented as the value after subtracting the lactate concentration in medium only.

Quantitative RT-PCR

Real-time quantitative RT-PCR (QPCR) was performed as previously described (Chang et al., 2009) using gene-specific primer sets (**Table S1**). The relative mRNA levels were assessed (in triplicate) based on normalization using a reference gene encoding β-Actin (Actb).

Retroviral transduction

Retroviral transduction was performed as previously described (Rivera-Walsh et al., 2000). HEK293T cells were transfected (by calcium method) with pCLXSN(GFP)-ASCT2 or pMIGR1-IRES-GFP-SNAT1 retroviral vectors along with the packaging vectors pCL-Eco (for naïve CD4 T cells) or pCL-Ampho (for Jurkat cells and JPM50.6 cells). Naive CD4 T cells ($CD4^+CD44^{lo}CD62L^{hi}$) were activated with plate-bound anti-CD3 (5 μg/mL) plus anti-CD28 (1 μg/mL) in 48-well plates for 30 hours and then infected with the packaged retroviruses. Transduced cells were used for *in vitro* T-cell differentiation and IP. The infected Jurkat cells and JPM50.6 cells were enriched by flow cytometric sorting based on GFP expression.

Imaging analysis

Jurkat cells and JPM50.6 cells were incubated in serum-free RPMI1640 medium overnight, and then stimulated for 15 min with anti-CD3 (OKT3) (1 μg/ml) and anti-CD28 (CD28.2) (1 μg/ml) that had been premixed with 10 μg/ml of a secondary crosslinking antibody: goat anti-mouse immunoglobulin G (H+L) (Jackson ImmunoResearch). The cells were fixed and permeabilized for 20 min with BD Cytofix/Cytoperm^{TM} solution (BD Bioscience) and washed then blocked in 0.5% bovine serum albumin (BSA) in PBS. Cells were then stained with primary antibody for ASCT2 (Millipore) and TCRβ (BD Bioscience) for 30 min, followed by staining with secondary AlexaFluor 488 or 647 antibodies (Molecular Probes) for 30 min. Samples were mounted in antifade reagent with 4′,6-Diamidino-2-phenylindole (DAPI). Pictures were taken by Leica SP5 RS confocal microscope and analysed by SlideBook 5.0 software.

Immunoblot (IB), immunoprecipitation (IP) analysis and electrophoretic mobility shift assay (EMSA)

For IB analysis, T cells were activated by anti-CD3 and anti-CD28 using the crosslinking method, and whole-cell lysates were prepared in a kinase cell-lysis buffer supplemented with phosphatase inhibitors (Uhlik et al., 1998) and were subjected to IB assays. For IP, T cells or transfected HEK293T cells were lysed in RIPA buffer. HA was isolated by immunoprecipitation and detected by IB using indicated antibodies. For EMSA, the T cells were stimulated with plate-bound anti-CD3 and anti-CD28, and nuclear extracts were prepared and analyzed by EMSA using ^{32}P-radiolabeled oligonucleotide probes as described (Ganchi et al., 1992; Schreiber et al., 1989). The oligonucleotide probes used were NF-kB, CAACGGCAGGGGAATTCCCCTCTCCTT; AP-1,

GATCTAGTGATGAGTCAGCCG; NFAT, TCGAGGAGGAAAAACTGTTTCATA; and NF-Y, AAGAGATTAACCAATCACGTACGGTCT.

T-cell transfer model of chronic colitis

$CD45RB^{hi}$ naïve CD4 T cells ($CD4^{+}CD25^{-}CD45RB^{hi}$) were purified from the spleen and lymph nodes of *Slc1a5*$^{+/+}$ or *Slc1a5*$^{-/-}$ mice by flow cytometric cell sorting. The purified naïve $CD4^{+}$ T cells (4 x 10^5 cells) were injected intravenously into RAG1-deficient mice (Chang et al., 2012). The recipient mice were monitored weekly for body weight changes. Some of the recipient mice were sacrificed at the indicated times for analyzing the Th1 and Th17 effector T cells in the mesentery lymph nodes.

***L. monocytogenes* infection**

Age- and sex-matched *Slc1a5*$^{+/+}$ and *Slc1a5*$^{-/-}$ mice (8 wk old) were infected i.v. with 2 x 10^4 colony-forming units of OVA-expressing recombinant *L. monocytogenes* (provided by Dr. Hao Shen, University of Pennsylvania). At day 7 post-infection, the mice were sacrificed for analysis of listeriolysin O (LLO)-specific $CD4^{+}$ effector T cells in the spleen. Briefly, splenocytes were stimulated for 6 h with 20 μg/ml of $LLO_{190\text{-}201}$ peptide (NEKYAQAYPNVS) in the presence of a protein transport inhibitor, monensin, and then subjected to intracellular IFN-γ staining and flow cytometry analysis. For T-cell adoptive transfer studies, $CD4^{+}$ T cells (4 x 10^6 cells) derived from *Slc1a5*$^{+/+}$ OT-II or *Slc1a5*$^{-/-}$ OT-II mice were injected i.v. into RAG-1-deficient mice, followed by i.v. injection of the OVA-expressing *L. monocytogenes* as described above. On day 7 post-infection, splenocytes were collected and stimulated for 6 h with the $OVA_{323\text{-}339}$ peptide (10 μg/ml)

(Genemed Synthesis) in the presence of monensin and then subjected to intracellular IFN-γ staining and flow cytometry analysis.

Induction and assessment of EAE.

Active EAE was induced by MOG_{35-55} immunization as described(Jin et al., 2009). For T-cell adoptive transfer experiments, $CD4^+$ T cells derived from wild-type or *Slc1a5*$^{-/-}$ mice were adoptively transferred i.v. into RAG1-deficient mice (1×10^7 cells/mouse). After 12-16 h, the recipient mice were immunized for EAE induction, monitored for disease severity, and subjected to flow cytometric analysis of the CNS and lymph node immune cells as described(Jin et al., 2009). Histological analysis was done as previously described (Xiao et al., 2013).

SUPPLEMENTARY REFERENCES

Buschdorf, J.P., Li Chew, L., Zhang, B., Cao, Q., Liang, F.Y., Liou, Y.C., Zhou, Y.T., and Low, B.C. (2006). Brain-specific BNIP-2-homology protein Caytaxin relocalises glutaminase to neurite terminals and reduces glutamate levels. J. Cell. Sci. *119*, 3337-3350.

Chang, J.H., Xiao, Y., Hu, H., Jin, J., Yu, J., Zhou, X., Wu, X., Johnson, H.M., Akira, S., Pasparakis, M.*, et al.* (2012). Ubc13 maintains the suppressive function of regulatory T cells and prevents their conversion into effector-like T cells. Nat. Immunol. *13*, 481-490.

Chang, M., Jin, W., Chang, J.H., Xiao, Y., Brittain, G.C., Yu, J., Zhou, X., Wang, Y.H., Cheng, X., Li, P.*, et al.* (2011). The ubiquitin ligase Peli1 negatively regulates T cell activation and prevents autoimmunity. Nat. Immunol. *12*, 1002-1009.

Chang, M., Jin, W., and Sun, S.C. (2009). Peli1 facilitates TRIF-dependent Toll-like receptor signaling and proinflammatory cytokine production. Nat. Immunol. *10*, 1089-1095.

Che, T., You, Y., Wang, D., Tanner, M.J., Dixit, V.M., and Lin, X. (2004). MALT1/paracaspase is a signaling component downstream of CARMA1 and mediates T cell receptor-induced NF-kappaB activation. J Biol Chem *279*, 15870-15876.

Finlay, D.K., Rosenzweig, E., Sinclair, L.V., Feijoo-Carnero, C., Hukelmann, J.L., Rolf, J., Panteleyev, A.A., Okkenhaug, K., and Cantrell, D.A. (2012). PDK1 regulation of mTOR and hypoxia-inducible factor 1 integrate metabolism and migration of CD8+ T cells. J. Exp. Med. *209*, 2441-2453.

Ganchi, P.A., Sun, S.-C., Greene, W.C., and Ballard, D.W. (1992). IκB/MAD-3 masks the nuclear localization signal of NF-κB p65 and acts with the C-terminal activation domain to inhibit NF-κB p65 DNA binding. Mol. Biol. Cell *3*, 1339-1352.

Hynes, J., Hill, R., and Papkovsky, D.B. (2006). The use of a fluorescence-based oxygen uptake assay in the analysis of cytotoxicity. Toxicol. In Vitro *20*, 785-792.

Jin, W., Zhou, X.F., Yu, J., Cheng, X., and Sun, S.C. (2009). Regulation of Th17 cell differentiation and EAE induction by the MAP3K NIK. Blood *113*, 6603-6610.

King, C.G., Kobayashi, T., Cejas, P.J., Kim, T., Yoon, K., Kim, G.K., Chiffoleau, E., Hickman, S.P., Walsh, P.T., Turka, L.A., and Choi, Y. (2006). TRAF6 is a T cell-intrinsic

negative regulator required for the maintenance of immune homeostasis. Nat. Immunol. *12*, 1088-1092.

Kung, H.N., Marks, J.R., and Chi, J.T. (2011). Glutamine synthetase is a genetic determinant of cell type-specific glutamine independence in breast epithelia. PLoS Genet. *7*, e1002229.

Reiley, W., Zhang, M., Wu, X., Graner, E., and Sun, S.-C. (2005). Regulation of the deubiquitinating enzyme CYLD by IkappaB kinase gamma-dependent phosphorylation. Mol. Cell. Biol. *25*, 3886-3895.

Reiley, W.W., Zhang, M., Jin, W., Losiewicz, M., Donohue, K.B., Norbury, C.C., and Sun, S.C. (2006). Regulation of T cell development by the deubiquitinating enzyme CYLD. Nat. Immunol. *7*, 411-417.

Rivera-Walsh, I., Cvijic, M.E., Xiao, G., and Sun, S.C. (2000). The NF-kappa B signaling pathway is not required for Fas ligand gene induction but mediates protection from activation-induced cell death. J. Biol. Chem. *275*, 25222-25230.

Schreiber, E., Matthias, P., Muller, M.M., and Schaffner, W. (1989). Rapid detection of octamer binding proteins with 'mini-extracts', prepared from a small number of cells. Nucl. Acids Res. *17*, 6419.

Uhlik, M., Good, L., Xiao, G., Harhaj, E.W., Zandi, E., Karin, M., and Sun, S.-C. (1998). NF-kappaB-inducing kinase and IkappaB kinase participate in human T-cell leukemia virus I Tax-mediated NF-kappaB activation. J. Biol. Chem. *273*, 21132-21136.

Wang, D., You, Y., Case, S.M., McAllister-Lucas, L.M., Wang, L., DiStefano, P.S., Nunez, G., Bertin, J., and Lin, X. (2002). A requirement for CARMA1 in TCR-induced NF-kappa B activation. Nat. Immunol. *3*, 830-835.

Xiao, Y., Jin, J., Chang, M., Chang, J.H., Hu, H., Zhou, X., Brittain, G.C., Stansberg, C., Torkildsen, O., Wang, X.*, et al.* (2013). Peli1 promotes microglia-mediated CNS inflammation by regulating Traf3 degradation. Nat. Med. *19*, 595-602.